Int J Adv Manuf Technol (2016) 86:2895–2904
DOI 10.1007/s00170-016-8383-0

ORIGINAL ARTICLE

Investigation on the effects of parameters on hot cracking and tensile shear strength of overlap joint in laser welding dissimilar Al alloys

Yulong Zhang[1,2,3] · **Fenggui Lu**[1,2,3] · **Haichao Cui**[1,2,3] · **Yan Cai**[1,2,3] · **Songtao Guo**[1,2,3] · **Xinhua Tang**[1,2,3]

Received: 18 July 2015 / Accepted: 13 January 2016 / Published online: 4 February 2016

Abstract With the increasing requirement for weight reduction in automotive industry, joining dissimilar aluminum (Al) alloys within overlap joint becomes more and more inevitable. However, hot cracking is a challenge issue in Al alloy welding. Overlap joint without hot cracking and also with good tensile shear strength is very important for industrial application. In order to better understand the hot cracking behavior in laser welding of dissimilar Al alloys, AA5754 and AA6013 sheets were overlap welded to investigate the effects of process parameters on hot cracking susceptibility, then the tensile shear tests were carried out on sound welded joint. The chemical composition, microstructure, and fusion ratio of welded joint were also studied. The results showed that the hot cracking can be prevented under appropriately choosing of welding process parameters. In particular, the critical process parameters to prevent the formation of hot cracking, i.e., welding speed 3.0, 3.3, 3.9, and 4.5 m/min with the corresponding overlap width 12, 10, 8, and 6 mm, were determined in the present study. The tensile shear strength of the sound welded joints without hot cracking reached 140 N/mm, which was qualified to meet the industrial application requirement.

Keywords Laser welding · Hot cracking · Al alloys · Overlap joint · Tensile shear strength

✉ Fenggui Lu
Lfg119@sjtu.edu.cn

[1] Shanghai Key Laboratory of Materials Laser Processing and Modification, Shanghai Jiao Tong University, 800 Dongchuan Road, Shanghai 200240, People's Republic of China

[2] Collaborative Innovation Center for Advanced Ship and Deep-Sea Exploration, Shanghai 200240, People's Republic of China

[3] School of Materials Science and Engineering, Shanghai Jiao Tong University, 800 Dongchuan Road, Shanghai 200240, People's Republic of China

1 Introduction

In recent years, with the increasing requirement of environmental protection and energy saving, light weighting and high fuel efficiency become one of the most important development directions [1–3]. The demand for weight reduction has driven increasing need for lightweight materials used in vehicles. Due to their attractive characteristics such as low density, high specific strength, and excellent mechanical properties, aluminum alloys have become one of the most important lightweight materials [4–6]. Among different Al alloys, the series 5000 (Al-Mg) and 6000 (Al-Mg-Si) are widely used in the fabrication of automotive, aircraft structures, and other structural applications [7–10]. As a critical joining technique for Al alloys, laser welding has been extensively applied in practical production because of its advantages such as high weld quality, high production rate, manufacturing flexibility, and low distortion [11–14]. However, welding of Al alloys is always accompanied by numerous welding defects including hot cracking, distortion, porosity in joints, etc. [15–17]. Especially, due to large solidification shrinkage, thermal tensions which generate tensions and deformations, and the sensitive chemical composition [18–21], hot cracking becomes one of the biggest challenges in Al alloy welding. Until now, a number of researches on welding of Al alloys have been carried out. Luijendijk [19] who conducted the welding of

dissimilar Al alloys found that the chemical composition of weld played an important role in hot cracking tendency, and the filler material can help avoid hot cracking efficiently for sheet thicknesses of 1.5 and 3 mm. Cicala et al. [22] studied the influence of welding speed on hot cracking in butt welding of Al alloy sheet and noticed that hot cracking sensitivity was strongly dependent on the welding speed, because the welding speed had an important influence on solidification speed and temperature gradient, and it can determine the deformation and tension of the molten pool during solidification. In the study of Park et al. [23], sheets of AA5052 and AA6061 with thickness of 2 mm were welded using friction stir welding (FSW) in butt joint. Because of the difference in Mg content of AA5052 and AA6061, the distribution of Mg in FSW joints of dissimilar Al alloys was studied by electron probe microanalysis (EPMA). As a result, no melting occurred during FSW and the material mixing patterns were clearly shown in FSW joints. Dong et al. [1, 24, 25] overlap-welded Al alloy sheet to stainless steel by gas tungsten arc welding (GTAW); the tensile shear test was conducted to estimate the strength of the overlap-welded joint. They found that the use of filler wire, the proper post-weld heat treatment, and ultrasonic vibration can help improve the joint strength significantly. The abovementioned studies reflected different aspects in hot cracking behavior in different welding conditions, and the others studied the welding of dissimilar alloys and the method to estimate the overlap-welded joint. However, few researchers investigated the hot cracking behavior in overlap joint of dissimilar Al alloys. Especially, because the thermal strain or displacement in welding can be strongly influenced by joint configuration, overlap-welded joint has a remarkably higher tendency to hot cracking than that of butt-welded joint when the sheet thickness is around 1 to 2 mm [26]. And also, overlap laser welding of dissimilar Al alloys has been applied in automotive industry gradually, so it is really crucial to provide guidance in prevention hot cracking as well as offer sound welded joint with high mechanical property.

To provide guidance for the prevention of hot cracking in overlap laser welding of dissimilar Al alloys, a lot of work have been performed. In our previous experiments, the influence of stacking order and laser power on hot cracking has been investigated [27] and found that the order of material stacking significantly affected weld's hot cracking susceptibility, and the critical laser power was obtained for tested conditions which could effectively reduce hot cracking. The present study focuses on the hot cracking behavior in laser welding of dissimilar Al alloys in different overlap width. Sheet of AA6013 was overlap-welded on the top of AA5754. The effects of the welding speed, overlap width, and the clamping condition on hot cracking were systematically investigated. The tensile shear strength of the welded joint without hot cracking was also examined. The chemical composition, microstructure, fusion ratio, and morphology were further discussed to provide guidance in overlap laser welding of dissimilar Al alloys.

Table 1 Chemical compositions of AA5754 and AA6013 used in the present study (wt%)

Alloy	Mg	Si	Fe	Cu	Mn	Cr	Zn	Al
AA5754	2.253	0.2437	0.2524	0.009	0.0675	0.1869	0.013	Bal
AA6013	1.023	0.6037	0.34	0.24	0.0218	0.19	0.0113	Bal

2 Experimental procedures

The base materials used in this investigation were AA5754 and AA6013; the chemical compositions of the two base materials are listed in Table 1. To investigate the effects of welding speed (V), overlap width (D), and clamping condition on hot cracking, sheets of AA5754 and AA6013 with dimension of 150 mm (L) × 100 mm (W) × 2 mm (t) were overlap-welded at different process parameters. Figure 1 illustrates the schematic of overlap-welded specimens, where D_S is the distance from the weld centerline to free edge, which is half of the overlap width in the test. Before welding, acetone was used to remove the oils that remained on the surface of the specimens. Then, sheets of Al alloys were welded by the fiber laser (Ytterbium laser system-10000) with an emission wavelength of 1070 nm and focused beam with a diameter of 0.6 mm and focal length of 300 mm. The laser beam focal position was on the top surface of upper sheet. The laser torch was inclined at

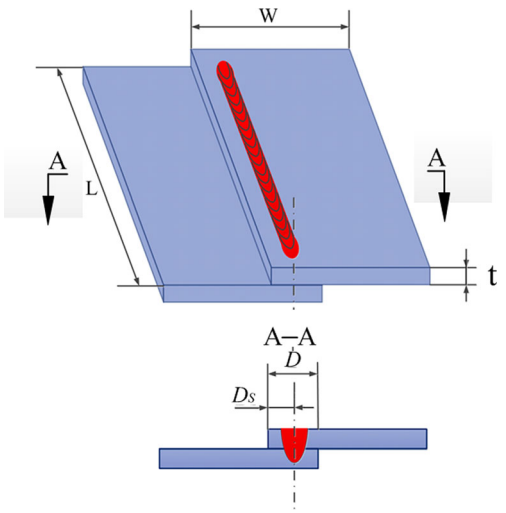

Fig. 1 The schematic of the overlap-welded sheets. The length (L), width (W), thickness (t), and overlap width (D) are marked

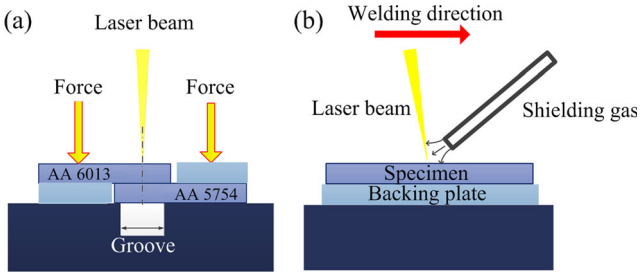

Fig. 2 The schematic of the welding process. **a** Front view. **b** Side view

an angle of 9° to prevent the burning damage caused by laser reflection from workpiece surface. Argon was used as shielding gas with a flow rate of 15 L/min supplied by a nozzle of 8 mm inner diameter, and the nozzle had an angle with horizontal direction of 40° to achieve a better protection effect. The backing sheet was also 2-mm-thick aluminum sheet. To avoid the distortion of the sheets which will form a gap between the interfaces, pressing force was applied on the sheets by clamping device before welding. The schematic of the welding setup is shown in Fig. 2.

To investigate the effects of welding speed and overlap width on hot cracking susceptibility, experiments with four different overlap widths of 12, 10, 8, and 6 mm were carried out, respectively. In order to guarantee the reliability of the experimental results, repeating tests were conducted for the same welding parameters. The welding parameters are listed in Table 2. In order to investigate the effect of clamping condition on hot cracking, two clamping condition being no constraint on free edge (NCFE) and with constraint on free edge (WCFE) were applied. At the WCFE condition, the pressure was applied on the free edge to decrease deformation due to the solidification shrinking and thermal tensions, as displayed in Fig. 3. After welding, the overlap-welded specimens were cut, mounted, polished, and prepared for metallographic analysis. The microstructure of the resultant welds was etched with Keller reagent, consisting of 1 % HF, 2.5 % HNO_3, 6.5 % HCl, and 90 % H_2O, and then observed by optical microscopy (OM, Leica-DM4000), and HBF_4 (2.5 % HBF_4) reagent was used for polarized light image. The distribution of the related elements was examined by energy-dispersive spectroscopy (EDS), and also the fracture surface of hot cracking was investigated by a scanning electron microscopy (SEM, JSM7600F).

Table 2 The results for cracking observation corresponding to different welding parameters used in the tests

D (mm)	12	10	8	6
V (m/min) and cracking appearance	2.7	3.0	3.6	4.2
	No	No	No	No
	3.0	3.3	3.9	4.5
	No	No	No	No
	3.3	3.6	4.2	4.8
	Yes	Yes	Yes	Yes
	3.6	3.9	4.5	5.1
	Yes	Yes	Yes	No

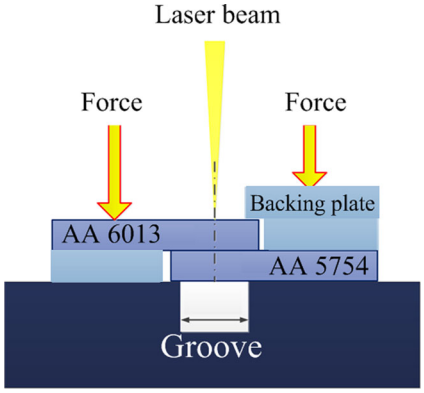

Fig. 3 The clamping condition (WCFE: with constraint in free edge) in which the download pressing load was applied on the free edge

The corresponding mechanical property of overlap-welded joint was evaluated through tensile shear test at room temperature. In order to estimate the tensile shear strength of the overlap joint without hot cracking, the tensile specimens were prepared for the tensile shear test (ISO 9018: 2003). The 25-mm-wide specimens were cut normally to each weld, and the joint was located in the center of the tensile specimen. For overlap-welded joint, two supporting sheets with the same thickness of the welding specimen (2 mm) were placed at each end of the tensile specimen, thus maintaining the joint region parallel to the tensile loading direction [28, 29]. Figure 4 shows the schematic of tensile specimen. All tests were conducted on Zwick/Roell Z100 testing machine at a constant speed of 1 mm/min. The failure load and failure location were

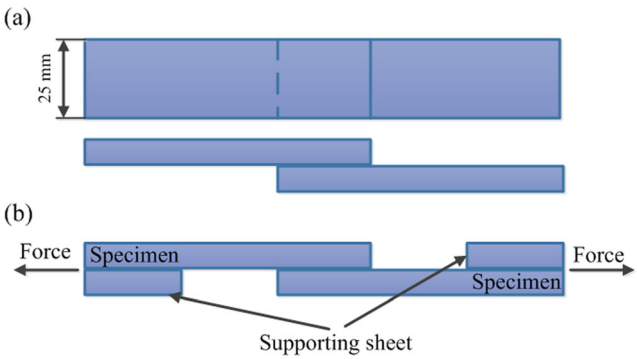

Fig. 4 The schematic of tensile shear specimen. **a** The 25-mm-wide tensile shear specimen. **b** Two supporting sheets were applied in the tensile shear test

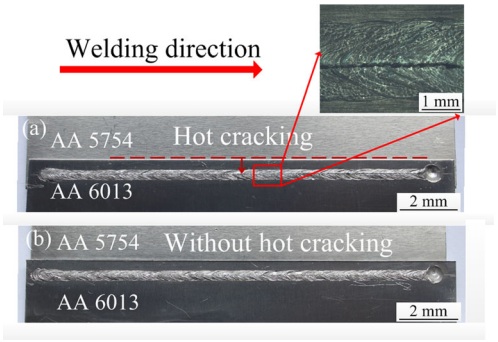

Fig. 5 Typical top view of the specimens. **a** $P = 4.50$ kW, $V = 3.6$ m/min, $D = 10$ mm, a long cracking exists on the surface. **b** $P = 4.50$ kW, $V = 3.3$ m/min, $D = 10$ mm, without visible cracking

recorded for each specimen. Two specimens for each welding parameter were tested to assure the repeatability, and the final failure loads were averaged.

3 Results and discussion

Generally, hot cracking occurs at the final stage of solidification when the material is under high temperature [30, 31]. Figure 5 shows the typical top view of the specimens after welding. In Fig. 5a, it can be observed that a long hot cracking occurs in the center of weld seam under the corresponding welding parameter. In Fig. 5b, the weld appearance is qualified without visible cracking.

3.1 The effect of welding speed and overlap width on hot cracking

The laser power was set as 4.5 kW to obtain proper penetration. In this test, the welding speed was changed for each overlap width. The welding parameters and cracking results are listed in Table 2. It shows that hot cracking susceptibility is different with respect to welding speed, and the increase of

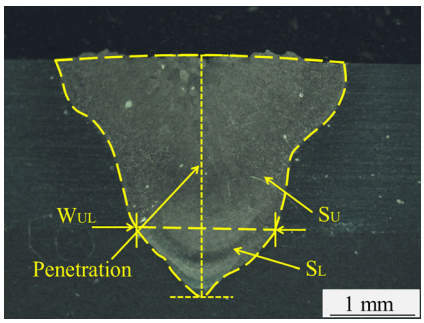

Fig. 6 The typical weld cross section, penetration, fusion ratio, and the weld width between upper and lower sheets (W_{UL}) were measured through cross section

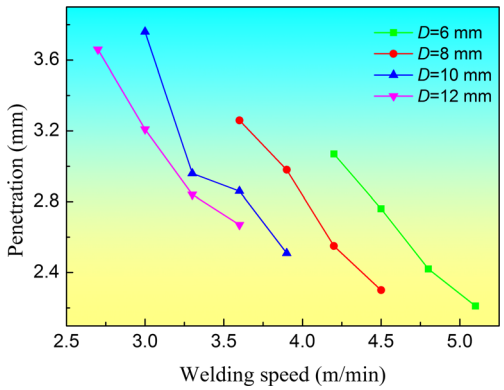

Fig. 7 Welding speed versus weld penetration of dissimilar joints of AA6013 and AA5754

welding speed causes large hot cracking susceptibility, namely changes from cracking free to cracking appearance.

After welding, the weld penetration and fusion ratio were measured on weld cross section. Figure 6 displays the typical weld cross section. Here, S_U and S_L are the fusion area of the upper and lower sheets, respectively. And fusion ratio R is defined as volumetric percentage of melted lower sheet with respect to the whole weld bead, given by:

$$R = \frac{S_L}{S_U + S_L} \tag{1}$$

The influence of welding speed on weld penetration of dissimilar joints is presented in Fig. 7. An obvious result is that decreasing the welding speed directly results in deeper penetration. In addition, the weld penetration increases significantly when the overlap width decreased. Figure 8 shows the influence of welding speed on fusion ratio of dissimilar joints. It shows that the tendency of fusion ratio with various welding speed is similar with that of weld penetration. With the increase of welding speed, the fusion ratio decreases.

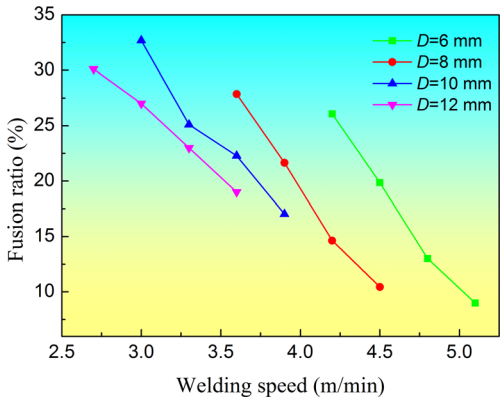

Fig. 8 Welding speed versus fusion ratio of dissimilar joints of AA6013 and AA5754

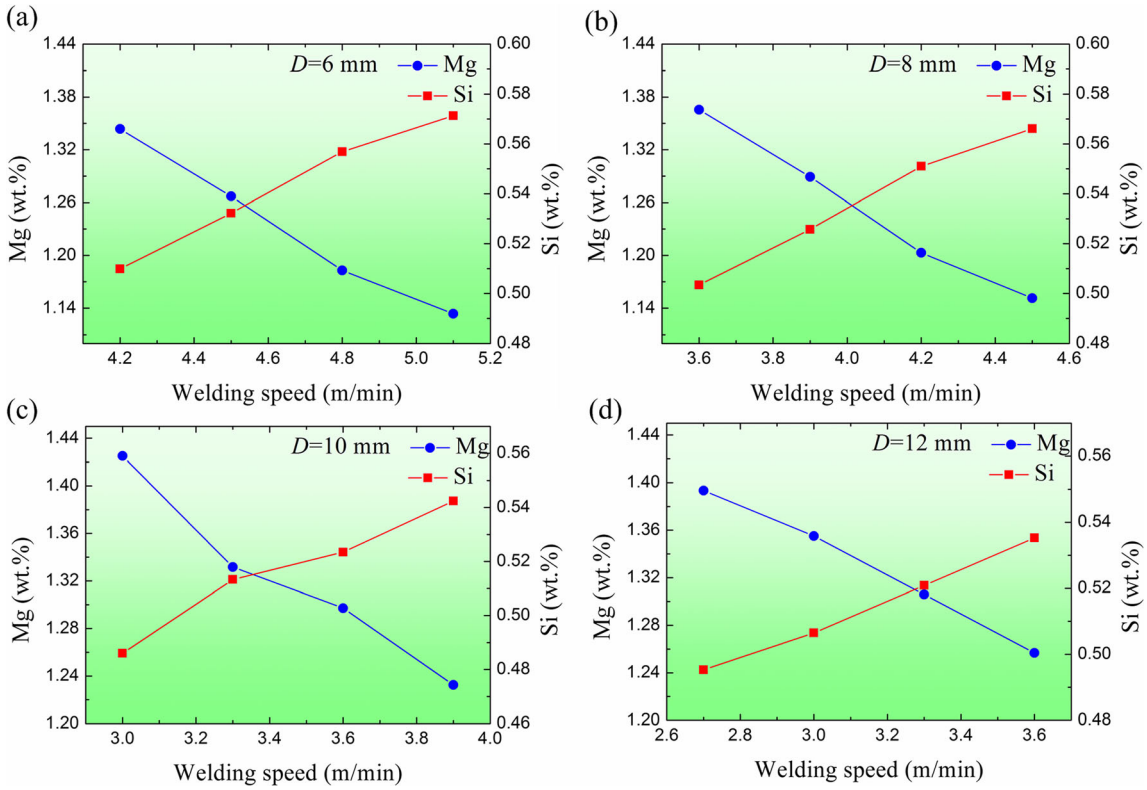

Fig. 9 The influence of welding speed on the average contents of Mg and Si in weld. **a** $D = 6$ mm. **b** $D = 8$ mm. **c** $D = 10$ mm. **d** $D = 12$ mm

It is known that hot cracking generally occurs at the final stage of solidification (the mushy zone where dendrites and the liquid phase coexist), the cavities between dendrites caused by either shrinkage or tensile stress are not able to be filled with the few remaining liquid film [26, 32]. The hot cracking susceptibility of weld is affected by both chemical compositions of the weld materials and the thermal and mechanical conditions the weld experiences during its solidification stage. When overlap welding of the same Al alloy sheets, the increase of welding speed will decrease the hot cracking susceptibility. As the welding speed slows down, the staying time of the mushy zone becomes longer; thus, the weld metal becomes easier to hot cracking [33]. However, due to use of dissimilar Al alloys in the present work, the tests showed different result. Actually, the hot cracking susceptibility depends greatly on the chemical composition of weld, especially the content of Mg and Si, during the welding of Al alloys. Hot cracking susceptibility reaches to the peak when chemical compositions of Si and Mg are around 0.62 and 0.86 wt%, respectively [22, 34]. Due to the overlap joint of dissimilar Al

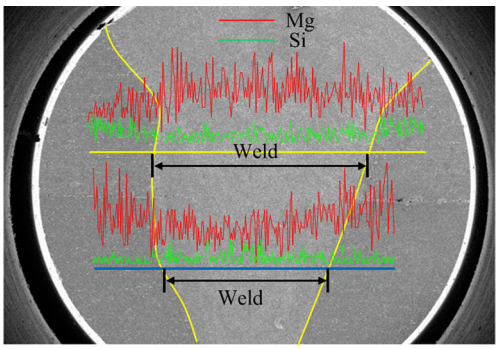

Fig. 10 The distribution of Mg and Si contents in EDS line scanning analysis along the *yellow line* in upper sheet and the *blue line* in lower sheet, respectively. Process parameters: $P = 4.5$ kW, $V = 3.0$ m/min, $D = 10$ mm

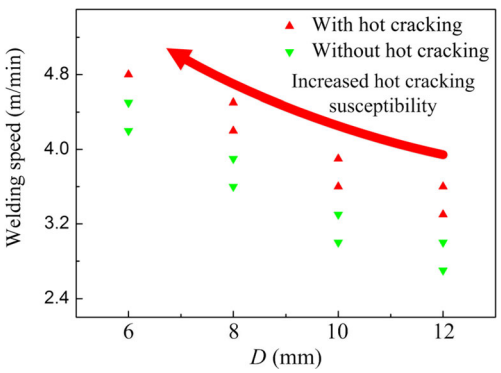

Fig. 11 The hot cracking susceptibility versus welding speed and overlap width

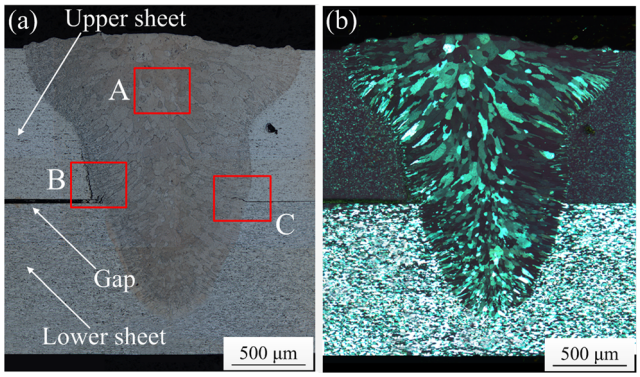

Fig. 12 The microstructure of the overlap joint without hot cracking in the surface with the welding speed 3.3 m/min and overlap width 10 mm. **a** Optical microscopy. **b** Microstructure in polarized light image

alloys, as the change of fusion ratio, the chemical compositions of weld will also change. The changing average content of Si and Mg in the weld due to the changing fusion ratio can be calculated as follows:

$$C_X = R \times C_{XL} + (1-R) \times C_{XU} \quad (2)$$

where C_X is the average content of element X, R is the fusion ratio, and C_{XL} and C_{XU} are the content of element X in AA5754 and AA6013 which are given in Table 1, respectively. Figure 9 exhibits the changing average contents of Mg and Si versus welding speed. It clearly shows that with the increase of welding speed, the contents of Mg and Si in the weld get closer to the highest hot cracking susceptibility.

The line scanning results of Mg and Si elements prove that these elements are mixed and redistributed in the weld after fusing by laser beam. Figure 10 displays the distribution of Mg and Si contents after welding. It can be found that the content of Mg in the weld is more than that in the base metal, namely AA6013 in the upper sheet along the yellow line. On the contrary, the content of Si decreases. Due to the different chemical compositions between upper and lower sheets, the distribution of Mg and Si along the blue line in the lower sheet shows the opposite result. As the mixture of different elements in weld, the chemical compositions of weld differ with each other due to the different welding speed. This explains that the hot cracking susceptibility increases as the welding speed increases, resulting in the variation of hot cracking from cracking free to cracking appearance.

The critical welding speeds are 3.0, 3.3, 3.9, and 4.5 m/min when the overlap widths are 12, 10, 8, and 6 mm, respectively. To avoid hot cracking, the welding speed should be less than these critical values. Besides, it can be found that when the overlap width is 6 mm, hot cracking disappears at the welding speed of 5.1 m/min. The lower sheet can hardly be welded to the upper sheet due to the high speed.

According to the experimental results, it was also found that as the overlap width decreases, the critical welding speed increases greatly as displayed in Fig. 11. Generally, owing to the thermal aggregation in the area between weld and free edge, the hot cracking easily occurs at the smaller overlap width. Due to thermal aggregation in the molten pool, large thermal stress would be induced by solidification shrinkage [30]. However, the fusion ratio will increase greatly at the smaller overlap width as illustrated in Fig. 8. This directly determines the chemical compositions of the weld. With the increase of the fusion ratio, element contents of Mg and Si within the weld vary from cracking sensitive values to non-sensitive ones, and thus the critical welding speed increases.

3.2 Microstructural analysis and the effect of clamping condition on hot cracking

3.2.1 Microstructural analysis

The typical microstructure of overlap laser welding dissimilar Al alloy joint is shown in Fig. 12. The grains in weld can be identified clearly by polarized light image, as revealed in Fig. 12b which is the same area with Fig. 12a. The grain structure in laser weld of overlap joint primarily consists of some equiaxed grains in the center and the columnar dendritic grains originating from the fusion line. Figures 13, 14, and 15 are partial enlarged detail microstructure of locations A, B, and C in Fig. 12, respectively. Figure 13b shows clearly the

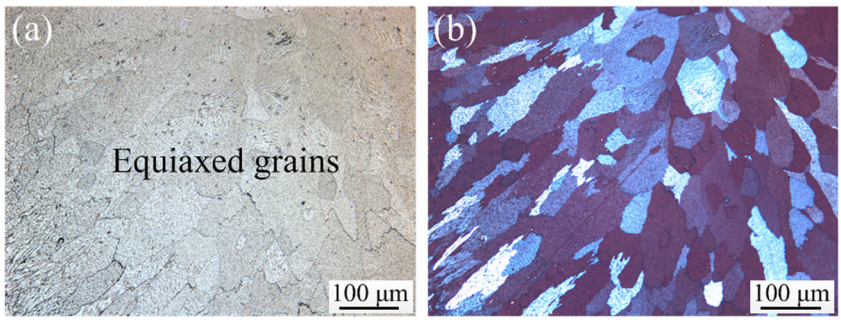

Fig. 13 Enlarged microstructure of equiaxed grains in location A of Fig. 12. **a** Optical microscopy. **b** Polarized light image

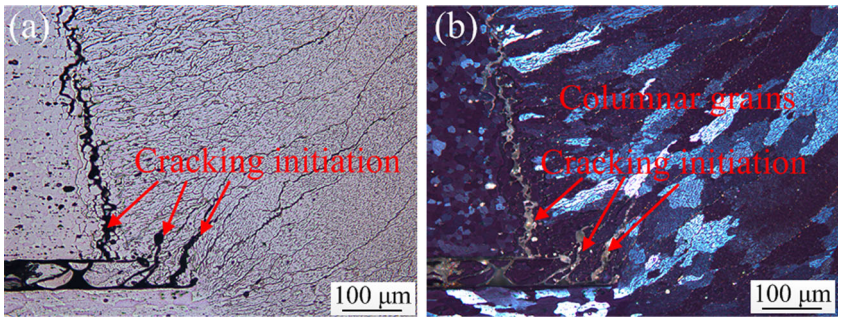

Fig. 14 Enlarged details of crack in location B of Fig. 12. **a** Optical microscopy. **b** Polarized light image

equiaxed grains in the center of weld. It can also be confirmed that the hot cracking initiates at intergranular in overlap weld and then propagates along the dendritic grain's boundary [35]. Figure 12 is the microstructure of overlap joint without hot cracking in the surface. Although there is no hot cracking in the surface, it still can be observed several short cracking at the cross corner of sheets. Figures 14 and 15 show that the cracking initiates from the fusion line between the upper and lower sheets and propagates along the dendritic grain's boundary. It is known that, in overlap-weld joint, stress and strain concentration exists at the gap between two sheets. The deformation of free edge results in the formation of the gap (see Fig. 12), at which the cracking easily initiates [33, 36], and then stops propagating as the chemical compositions of weld not sensitive to hot cracking.

3.2.2 The effect of clamping condition on hot cracking

Based on the abovementioned discussion, the deformation of free edge due to thermal shrinkage leads to the cracking initiation, and the propagation of the cracking depends on the chemical compositions of the weld. One way to avoid the hot cracking is to control the chemical compositions of the weld, and the other way is to decrease the deformation of the free edge by applying constraint, as displayed in Fig. 3. To investigate the effect of constraint condition in overlap joint configuration on hot cracking, experiments under same welding parameter with respect to different constraint condition were carried out. The welding parameters and the results for cracking observation are listed in Table 3.

The results of this investigation show that the satisfactory weld without hot cracking can be produced by applying pressing force on the free edge. The same welding parameter results in the same thermal shrinkage and chemical compositions of weld. However, the pressing force on free edge can decrease its upwarp hence producing the hot cracking free weld.

3.3 SEM observation

The hot cracking can be elucidated by the observations of the fractures. As occurs in the fusion zone during solidification of the weld pool, hot cracking is characterized by a dendritic fracture surface [37]. Figure 16 shows the fracture surface characteristic of the phenomenon of hot cracking in laser welding. The smooth surface of grains indicates that the hot cracking originates during the solidification process which is at high temperature. Some theories of hot cracking indicate that the hot cracking propagates through the liquid film covering grain boundaries [38, 39]. Due to the thermal shrinkage and inadequate filled with liquid, the hot cracking easily occurs [35].

3.4 Tensile shear testing

Based on the results and discussion above, as the welding speed decreases, the hot cracking susceptibility reduces during

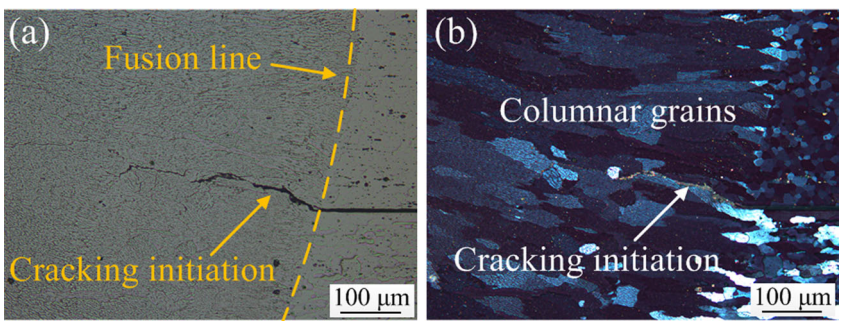

Fig. 15 Enlarged details of crack in location C of Fig. 12. **a** Optical microscopy. **b** Polarized light image

Table 3 Welding parameters used in the tests

D (m)		12	12	10	10	8	8
V (m/min)		3.3	3.6	3.6	3.9	4.2	4.5
Cracking	NCFE	Yes	Yes	Yes	Yes	Yes	Yes
	WCFE	No	No	No	No	No	No

NCFE no constraint on free edge, *WCFE* with constraint on free edge

the overlap laser welding of dissimilar Al alloy sheets. The sound weld joint without hot cracking can be produced when the welding speed is no more than the critical values at each overlap width. Generally, the tensile shear strength of overlap-welded joint is one of the important mechanical properties [1, 40, 41]. Some researchers have studied the overlap joint shear property of Al alloys series 5000 and 6000 sheets welded by FSW [42] and friction stir spot welding (FSSW) [43, 44]. In this study, the tensile shear test was carried out for these welds free from hot cracking. The effect of welding speed on tensile shear load of overlap-welded joints of dissimilar Al alloys is shown in Fig. 17. As described before, the specimen for tensile shear test has a width of 25 mm, so here the characteristic value of tensile shear (special tensile shear strength) was calculated as the maximum load divided by the specimen width. As illustrated in Fig. 17, the tensile shear load decreases as the welding speed increases at constant overlap width. The greatest shear strength (172 N/mm) was obtained under the following welding condition: overlap width 10 mm and

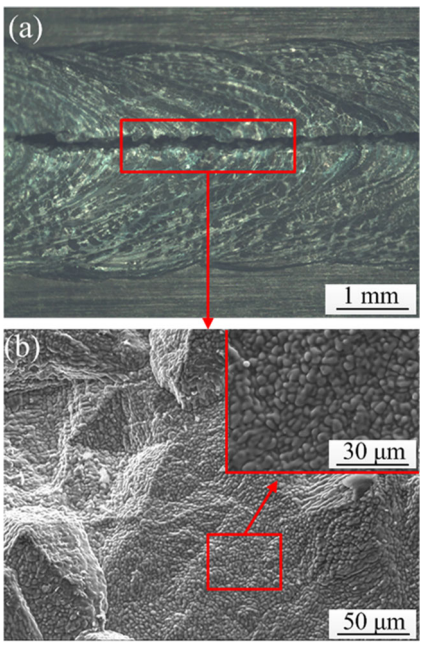

Fig. 16 Hot cracking fracture morphology in laser welding. **a** Macrograph top view. **b** Details of fracture surface

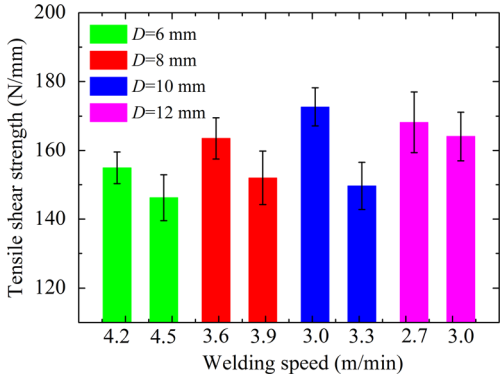

Fig. 17 The effect of welding speed on fracture load in tensile shear testing

welding speed 3 m/min. Compared with the shear strength of joint made by FSW and FSSW joints (less than 120 N/mm), the shear strength value of the joint produced by laser welding (approximately 140 N/mm) was higher. The tensile shear strength of overlap joint depends on the area between upper and lower sheets, which can be calculated by the weld width between upper and lower sheets (W_{UL}) multiplies the specimen's width (25 mm). The measurement of the W_{UL} in cross section of weld as illustrated in Fig. 6. Table 4 lists the value of W_{UL} and corresponding welding speeding and overlap width. It can be found that the weld width between upper and lower sheets decreases as welding speed increases, which can explain the decrease of tensile shear strength.

4 Conclusions

The effects of welding speed, overlap width, and clamping condition on hot cracking susceptibility of laser welding of dissimilar Al alloys in overlap joint were investigated. The sound joint free from hot cracking could be produced if the welding parameters were appropriately chosen. From this research, the following conclusions can be obtained:

1. With the increase of welding speed, the hot cracking susceptibility increases. The critical welding speed was 3.0, 3.3, 3.9, and 4.5 m/min when the overlap width was set as 12, 10, 8, and 6 mm, respectively. To avoid the formation

Table 4 The weld width between upper and lower sheets (W_{UL}) under different welding parameters

D (mm)	6	6	8	8	10	10	12	12
V (m/min)	4.2	4.5	3.6	3.9	3.0	3.3	2.7	3.0
W_{UL} (mm)	1.67	1.53	1.90	1.81	2.04	1.57	1.89	1.79

of hot cracking, welding speed should be less than these thresholds.
2. The fusion ratio increased greatly as overlap width reduced from 12 to 6 mm, resulting in the increase of critical welding speed.
3. The deformation of free edge due to the thermal shrinkage easily leads to the initiation of cracking, and sound weld without hot cracking can be produced by applying constraint on the free edge.
4. The tensile shear strength of the joints without hot cracking was more than 140 N/mm, which meets the industrial application requirement.

Acknowledgments The authors gratefully acknowledge the financial support by the National Natural Science Foundation of China (Grant No. 51204109).

References

1. Dong HG, Yang LQ, Dong C, Kou S (2010) Arc joining of aluminum alloy to stainless steel with flux-cored Zn-based filler metal. Mater Sci Eng A 527:7151–7154
2. Liu X, Lan S, Ni J (2014) Analysis of process parameters effects on friction stir welding of dissimilar aluminum alloy to advanced high strength steel. Mater Des 59:50–62
3. Jonckheere C, Meester BD, Cassiers C, Delhaye M, Simar A (2012) Fracture and mechanical properties of friction stir spot welds in 6063-T6 aluminum alloy. Int J Adv Manuf Technol 62:569–575
4. Miller W, Zhuang L, Bottema J, Wittebrood AJ, De Smet P, Haszler A, Vieregee A (2000) Recent development in aluminium alloys for the automotive industry. Mater Sci Eng A 280:37–49
5. Sutton M, Yang B, Reynolds A, Taylor R (2002) Microstructural studies of friction stir welds in 2024-T3 aluminum. Mater Sci Eng A 323:160–166
6. Zhang XH, Chen GY, An WK, Deng ZH, Zhou ZX (2014) Experimental investigations of machining characteristics of laser-induced thermal cracking in alumina ceramic wet grinding. Int J Adv Manuf Technol 72:1325–1331
7. Haghayeghi R, Zoqui EJ, Bahai H (2009) An investigation on the effect of intensive shearing on the grain refinement of A5754 aluminium alloy. J Alloy Compd 481:358–364
8. Suhuddin U, Fischer V, Kroeff F, dos Santos JF (2014) Microstructure and mechanical properties of friction spot welds of dissimilar AA5754 Al and AZ31 Mg alloys. Mater Sci Eng A 590:384–389
9. Lakshminarayanan AK, Balasubramanian V, Elangovan K (2009) Effect of welding processes on tensile properties of AA6061 aluminium alloy joints. Int J Adv Manuf Technol 40:286–296
10. Kasman Ş, Yenier Z (2014) Analyzing dissimilar friction stir welding of AA5754/AA7075. Int J Adv Manuf Technol 70:145–156
11. Jia J, Yang SL, Ni WY, Bai JY (2014) Microstructure and mechanical properties of fiber laser welded joints of ultrahigh-strength steel 22MnB5 and dual-phase steels. J Mater Res 29:2565–2575
12. Haboudou A, Peyre P, Vannes A, Peix G (2003) Reduction of porosity content generated during Nd:YAG laser welding of A356 and AA5083 aluminium alloys. Mater Sci Eng A 363:40–52
13. Sathiya P, Jaleel MYA (2011) Influence of shielding gas mixtures on bead profile and microstructural characteristics of super austenitic stainless steel weldments by laser welding. Int J Adv Manuf Technol 54:525–535
14. Li C, Liu L (2013) Investigation on weldability of magnesium alloy thin sheet T-joints: arc welding, laser welding, and laser-arc hybrid welding. Int J Adv Manuf Technol 65:27–34
15. Koilraj M, Sundareswaran V, Vijayan S, Koteswara Rao SR (2012) Friction stir welding of dissimilar aluminum alloys AA2219 to AA5083—optimization of process parameters using Taguchi technique. Mater Des 42:1–7
16. Chino Y, Iwasaki H, Mabuchi M (2004) Cavity growth rate in superplastic 5083 Al and AZ31 Mg alloys. J Mater Res 19:3382–3388
17. Zhang H, Wang S (2012) A first-principles study on hot crack mechanism in Mg-Al-Ca alloys. J Mater Res 27:1631–1637
18. Mai TA, Spowage AC (2004) Characterisation of dissimilar joints in laser welding of steel–kovar, copper–steel and copper–aluminium. Mater Sci Eng A 374:224–233
19. Luijendijk T (2000) Welding of dissimilar aluminium alloys. J Mater Process Tech 103:29–35
20. Behler K, Berkmanns J, Ehrhardt A, Frohn W (1997) Laser beam welding of low weight materials and structures. Mater Des 18:261–267
21. Balasubramanian V, Ravisankar V, Reddy GM (2008) Effect of pulsed current welding on mechanical properties of high strength aluminum alloy. Int J Adv Manuf Technol 36:254–262
22. Cicală E, Duffet G, Andrzejewski H, Grevey D, Ignat S (2005) Hot cracking in Al–Mg–Si alloy laser welding—operating parameters and their effects. Mater Sci Eng A 395:1–9
23. Park SK, Hong ST, Park JH, Park KY, Kwon YJ, Son HJ (2010) Effect of material locations on properties of friction stir welding joints of dissimilar aluminium alloys. Sci Technol Weld Joi 15:331–336
24. Dong H, Liao C, Yang L, Dong C (2012) Effects of post-weld heat treatment on dissimilar metal joint between aluminum alloy and stainless steel. Mater Sci Eng A 550:423–428
25. Dong HG, Yang LQ, Dong C, Kou S (2012) Improving arc joining of Al to steel and Al to stainless steel. Mater Sci Eng A 534:424–435
26. Cao X, Wallace W, Immarigeon JP, Poon C (2003) Research and progress in laser welding of wrought aluminum alloys. II. Metallurgical microstructures, defects, and mechanical properties. Mater Manuf Process 18:23–49
27. Zhang YL, Lu FG, Wang HP, Wang XJ, Cui HC, Tang XH (2015) Reduced hot cracking susceptibility by controlling the fusion ratio in laser welding of dissimilar Al alloys joints. J Mater Res 30:993–1001
28. Lathabai S, Painter MJ, Cantin GMD, Tyagi VK (2006) Friction spot joining of an extruded Al–Mg–Si alloy. Scripta Mater 55:899–902
29. AWS D1/D1: Code, (1985).
30. Wang J, Wang HP, Wang X, Cui HC, Lu FG (2015) Statistical analysis of process parameters to eliminate hot cracking of fiber laser welded aluminum alloy. Opt Laser Technol 66:15–21
31. Hu B, Richardson IM (2006) Mechanism and possible solution for transverse solidification cracking in laser welding of high strength aluminium alloys. Mater Sci Eng A 429:287–294
32. Eskin DG, Suyitno KL (2004) Mechanical properties in the semi-solid state and hot tearing of aluminium alloys. Prog Mater Sci 49:629–711

33. Wang XJ, Wang HP, Lu FG, Carlson BE, Wu YX (2014) Analysis of solidification cracking susceptibility in side-by-side dual-beam laser welding of aluminum alloys. Int J Adv Manuf Tech 73:73–85
34. Cao G, Kou S (2006) Predicting and reducing liquation-cracking susceptibility based on temperature vs fraction solid. Weld J 85:9–18
35. Böllinghaus T, Herold H, Cross CE, Lippold JC (2008) Hot cracking phenomena in welds. Springer, Berlin, p 247
36. Kong F, Kovacevic R (2010) 3D finite element modeling of the thermally induced residual stress in the hybrid laser/arc welding of lap joint. J Mater Process Tech 210:941–950
37. Lippold J, Böllinghaus T, Cross CE (2011) Hot cracking phenomena in welds. Springer, Berlin, p 95
38. Eskin DG, Katgerman L (2007) A quest for a new hot tearing criterion. Metall Mater Trans A 38:1511–1519
39. Rappaz M, Drezet JM, Gremaud M (1999) A new hot-tearing criterion. Metall Mater Trans A 30:449–455
40. Cao R, Huang Q, Chen JH, Wang PC (2014) Cold metal transfer spot plug welding of AA6061-T6-to-galvanized steel for automotive applications. J Alloy Compd 585:622–632
41. Saeid T, Abdollah-zadeh A, Sazgari B (2010) Weldability and mechanical properties of dissimilar aluminum–copper lap joints made by friction stir welding. J Alloy Compd 490:652–655
42. Lee CY, Lee WB, Kim JW, Choi DH, Yeon YM, Jung SB (2008) Lap joint properties of FSWed dissimilar formed 5052 Al and 6061 Al alloys with different thickness. J Mater Sci 43:3296–3304
43. Uematsu Y, Tokaji K, Tozaki Y, Kurita T, Murata S (2008) Effect of re-filling probe hole on tensile failure and fatigue behaviour of friction stir spot welded joints in Al–Mg–Si alloy. Int J Fatigue 30:1956–1966
44. Fujimoto M, Watanabe D, Abe N, Yutaka SS, Kokawa H (2010) Effects of process time and thread on tensile shear strength of Al alloy lap joint produced by friction stir spot welding. Weld Int 24:169–175